

# Theory and Experiment of the Cavity-Backed Slot-Excited Dielectric Resonator Antenna

Kut Yuen Chow and Kwok Wa Leung, *Member, IEEE*

**Abstract**—A slot-excited hemispherical dielectric resonator antenna backed by a rectangular cavity is studied theoretically and experimentally. The magnetic-type dyadic Green's function for the rectangular cavity is derived using the mode-matching method. An integral equation for the equivalent magnetic current is obtained by enforcing the boundary condition across the slot. The moment method with the Galerkin's procedure is then used to find the magnetic current in the slot and, hence, the input impedance of the antenna. Measurements were carried out to verify the theory and good agreement is obtained. The effects of the slot inclination angle, of the slot offset, and of the cavity size on the input impedance are discussed.

**Index Terms**—Cavity resonators, dielectric antennas, mode-matching methods, moment methods.

## I. INTRODUCTION

A DIELECTRIC resonator has no conductor loss and can be used as an efficient antenna, namely the dielectric resonator antenna (DRA) [1]–[3]. With the advantages of small size, high radiation efficiency, and relatively large impedance bandwidth, the DRA is very suitable for modern communications. Among the various excitation schemes [4]–[8] for the DRA, the slot fed by a microstripline [8] is often used to excite the DRA. Recently, A. A. Kishk *et al.* [6] reported a modified structure in which the microstripline beneath the slot is replaced by free-space, with excitation modeled by a delta-gap source. This modified configuration has advantages of being relatively simple to build and analyze. However, it always produces undesirable backside radiation, which should be avoided in the electromagnetic compatibility (EMC) design. A remedy to this problem is to cover the back of the slot by a metallic cavity.

The cavity-backed slot (CBS) antenna (without the DRA) has been well studied in the literature [9]–[15]. The first theoretical analysis of the CBS antenna was introduced by Galejs [9], who expanded the fields within a rectangular hollow waveguide by modal terms. The waveguide was shorted at both ends by two conducting planes, one of which contained the slot. He enforced the boundary condition of the magnetic field across the slot and found the admittance of the CBS antenna using the variational method. Cockrell [10] and Li *et al.* [11] employed the complex Poynting theorem to calculate the input admittances of the rectangular and cylindrical CBS antennas, respectively. The fields external and internal to the cavity were derived. Use was made of conservation of energy to equate the input power to the power

delivered to the cavity and free-space. In this method, the aperture field was modeled by a single current term, which is not accurate especially at high frequencies. Hadidi and Hamid [12] and Leung and Chow [13] performed similar work by using the method of moments (MoM). Extensive measurements were carried out by Long [14] for the rectangular CBS antenna, based on which a mathematical model [15] was developed. Recently, Biebl and Friedsam [16] have employed layers of dielectric and magnetic substrates to cover the CBS antenna to improve the radiation efficiency, pattern shape, and antenna gain. However, no information of the CBS excited DRA has been available in the literature.

In this paper, the rectangular CBS excited hemispherical DRA is studied theoretically and experimentally. The hemispherical DRA is excited at the fundamental broadside  $TE_{111}$  mode [8]. So far, analysis of the rectangular CBS structure has been limited to the configuration that the slot is aligned with the cavity edge. A more general case in which the slot has an arbitrary inclination angle is considered in this paper. The Green's function approach is used to formulate an integral equation for the slot current, which is solved using the MoM. The Green's function of the hemispherical DRA in the upper-half plane has been well studied [8] and will not be discussed in detail. For the cavity part, the mode-matching method is used to rigorously derive the magnetic-type dyadic Green's function due to a magnetic point current. To save computation time, the integration of the impedance elements involving the cavity Green's function is performed analytically. The theory agrees very well with experiment. In this paper, the effects of the slot inclination angle, of the slot offset, and of the cavity size on the input impedance are investigated. Finally, the equivalent magnetic current in the slot is calculated and discussed.

## II. FORMULATION

Fig. 1 shows the geometry of the CBS excited DRA. A slot of length  $L$  and width  $W$  cut from a thin infinite ground plane is mounted onto a rectangular metallic cavity. The width, length, and depth of the cavity are  $a$ ,  $b$ , and  $c$ , respectively, whereas the radius and dielectric constant of the hemispherical DRA are  $a_r$  and  $\epsilon_r$ , respectively. The slot is located at the center of the DRA so that excitation of the DRA  $TE_{111}$  mode is strongest [8]. The slot is inclined at an angle  $\phi_{in}$  from the  $x$ -axis, with offsets  $x_d$  and  $y_d$  from the  $y$ - and  $x$ -axes, respectively. In the following formulation, the fields are assumed to vary harmonically as  $e^{j\omega t}$ , which is suppressed throughout the paper. Furthermore, the primed and unprimed position vectors denote the source and field points, respectively. Since the slot is slender ( $k_\epsilon W \ll 1$ ,  $W \ll L$ ), the transverse current component  $M'_\xi$  is

Manuscript received April 16, 1999; revised April 5, 2000. This work was supported by a RGC Research Grant.

The authors are with the Department of Electronic Engineering, City University of Hong Kong, Kowloon Tong, Kowloon, Hong Kong.

Publisher Item Identifier S 0018-9375(00)06644-8.

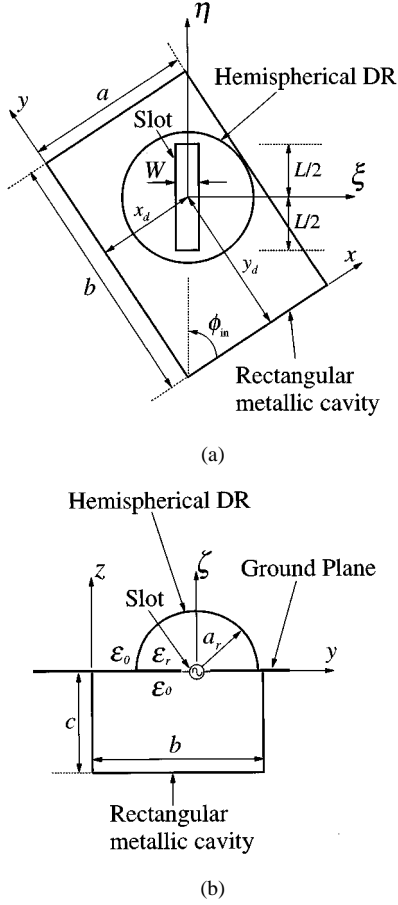


Fig. 1. The geometry of the cavity-backed slot-excited DRA. (a) Top view. (b) Side view.

neglected and only the longitudinal component  $M_\eta$  is considered in this paper. The slot is excited at  $\eta = \eta_0$ .

To begin with, the following boundary condition for the magnetic field is enforced across the slot ( $\zeta = 0$ )

$$H_\eta^+ - (-H_\eta^-) = I_0 \delta(\eta - \eta_0) \quad (1)$$

where “+” and “-” denote the fields just above and below the ground plane, respectively and  $I_0$  the terminal current of the excitation source. In terms of the DRA and cavity Green’s functions, (1) can be written as

$$-\iint_{S_0} [2G_a(\xi, \eta; \xi', \eta') + G_c(\xi, \eta; \xi', \eta')] M_\eta(\eta') ds' = I_0 \delta(\eta - \eta_0) \quad (2)$$

where  $G_a$  and  $G_c$  are the DRA and rectangular cavity Green’s functions, respectively, and  $S_0$  is the surface of the slot. The factor of two associated with  $G_a$  accounts for the presence of the ground plane. Using the MoM, the magnetic current  $M_\eta(\eta)$  is expanded using a set of piecewise sinusoidal (PWS) basis functions  $f_n(\eta)$

$$M_\eta(\eta) = \frac{1}{W} \sum_{n=1}^N V_n f_n(\eta) \quad (3)$$

where

$$f_n(\eta) = \begin{cases} \frac{\sin[k_e(d - |\eta - \eta_n|)]}{\sin k_e d} & \eta_n - d < \eta < \eta_n + d \\ 0 & \text{elsewhere} \end{cases} \quad (4)$$

in which  $k_e = k_0 \sqrt{(1 + \epsilon_r)/2}$ ,  $\eta_n = -L/2 + n d$ ,  $d = L/(N + 1)$ , and  $V_n$  are unknown coefficients to be determined. Insertion of (3) into (2) yields

$$-\frac{1}{W} \sum_{n=1}^N V_n \iint_{S_0} [2G_a(\xi, \eta; \xi', \eta') + G_c(\xi, \eta; \xi', \eta')] f_n(\eta') ds' = I_0 \delta(\eta - \eta_0). \quad (5)$$

For convenience, the terminal current  $I_0$  is assumed to be unity. Using the Galerkin’s procedure, (5) is transformed into a matrix equation from which the unknown coefficients  $V_n$  can be solved

$$[2Y_{mn}^a + Y_{mn}^c] [V_n] = [f_n(\eta_0)] \quad m, n = 1, 2, \dots, N \quad (6)$$

where

$$Y_{mn}^{a,c} = \frac{-1}{W} \iint_{S_0} \iint_{S_0} f_m(\eta) G_{a,c}(\xi, \eta; \xi', \eta') f_n(\eta') ds ds' \quad (7)$$

The Green’s function  $G_a$  and its associated admittance  $Y_{mn}^a$  have been well studied [8] and therefore are omitted in this paper. Instead, the cavity Green’s function  $G_c$  and the cavity admittance  $Y_{mn}^c$  will be given in the next section. Once the unknown coefficients  $V_n$  are found, the input impedance of the antenna  $Z_{in}$  is obtained easily by using

$$Z_{in} = W M_\eta(\eta_0) = \sum_{n=1}^N V_n f_n(\eta_0). \quad (8)$$

### III. DERIVATION OF $G_c$ AND $Y_{mn}^c$

For convenience, the derivation of the Green’s function  $G_c$  will be carried out in the  $\vec{r}(x, y, z)$  coordinates, where the  $\vec{r}(x, y, z)$  and  $\vec{r}(\xi, \eta, z)$  coordinates are related as follows:

$$x = x_d + \xi \sin \phi_{in} + \eta \cos \phi_{in} \quad (9)$$

$$y = y_d - \xi \cos \phi_{in} + \eta \sin \phi_{in} \quad (10)$$

$$z = \zeta. \quad (11)$$

The magnetic current  $M_\eta(\eta')$  in the slot is first resolved into the  $M_x(x')$  and  $M_y(y')$  components as follows:

$$M_x(x') = M_\eta(\eta') \cos \phi_{in} \quad (12)$$

$$M_y(y') = M_\eta(\eta') \sin \phi_{in}. \quad (13)$$

These currents produce  $H_x$  and  $H_y$ . Mathematically

$$H_{x,y} = \iint_{S_0} \left[ G_{M_x}^{H_{x,y}}(x, y; x', y') M_x(x') + G_{M_y}^{H_{x,y}}(x, y; x', y') M_y(y') \right] ds' \quad (14)$$

where  $G_{M_\alpha}^{H_\beta}(\alpha, \beta = x, y)$  are magnetic-field Green's functions of the rectangular cavity and will be derived in the next part. The magnetic fields  $H_x$  and  $H_y$  are then combined to form the magnetic field  $H_{\eta}^-$  in (1)

$$H_{\eta}^- = H_x \cos \phi_{\text{in}} + H_y \sin \phi_{\text{in}}. \quad (15)$$

Subsequently,  $G_c$  is found as follows:

$$\begin{aligned} G_c = & \left[ G_{M_x}^{H_x}(x, y; x', y') \cos \phi_{\text{in}} \right. \\ & + \left. G_{M_y}^{H_x}(x, y; x', y') \sin \phi_{\text{in}} \right] \cos \phi_{\text{in}} \\ & + \left[ G_{M_x}^{H_y}(x, y; x', y') \cos \phi_{\text{in}} \right. \\ & + \left. G_{M_y}^{H_y}(x, y; x', y') \sin \phi_{\text{in}} \right] \sin \phi_{\text{in}}. \quad (16) \end{aligned}$$

Note that  $G_c$  can be reduced to simple forms  $G_{H_x}^{M_x}(x, y; x', y') \cos^2 \phi_{\text{in}}$  and  $G_{H_y}^{M_y}(x, y; x', y') \sin^2 \phi_{\text{in}}$  for  $\phi_{\text{in}} = 0$  and  $\pi/2$ , respectively.

#### A. Green's Functions $G_{M_x}^{H_x}$ , $G_{M_y}^{H_x}$ , $G_{M_x}^{H_y}$ and $G_{M_y}^{H_y}$

Using the boundary condition that the tangential electric field is zero on the interior surface of the cavity, it is straightforward to solve the following differential equation by using the Tai's procedure [17]:

$$\begin{aligned} \nabla \times \nabla \times \bar{\bar{G}}_M^{\bar{H}}(\vec{r}, \vec{r}') - k_0 \bar{\bar{G}}_M^{\bar{H}}(\vec{r}, \vec{r}') \\ = -j\omega\epsilon_0 \bar{\bar{I}}\delta(\vec{r} - \vec{r}') \quad (17) \end{aligned}$$

where  $\bar{\bar{G}}_M^{\bar{H}}$  and  $\bar{\bar{I}}$  are the magnetic type dyadic Green's functions in the rectangular cavity and the idem factor, respectively. Once  $\bar{\bar{G}}_M^{\bar{H}}$  is solved, the Green's functions  $G_{M_x}^{H_x}$ ,  $G_{M_y}^{H_x}$ ,  $G_{M_x}^{H_y}$ , and  $G_{M_y}^{H_y}$  can be found from the components of  $\bar{\bar{G}}_M^{\bar{H}}$  and are given as follows:

$$\begin{aligned} G_{M_x}^{H_x}(x, y; x', y') = & - \sum_{p=1}^{\infty} \sum_{q=0}^{\infty} C_1 \epsilon_q (k_0^2 - k_x^2) \sin(k_x x) \\ & \times \sin(k_x x') \cos(k_y y) \cos(k_y y') \quad (18) \end{aligned}$$

$$\begin{aligned} G_{M_y}^{H_x}(x, y; x', y') = & \sum_{p=1}^{\infty} \sum_{q=1}^{\infty} C_1 (k_x k_y) \sin(k_x x) \\ & \times \cos(k_x x') \cos(k_y y) \sin(k_y y') \quad (19) \end{aligned}$$

$$\begin{aligned} G_{M_x}^{H_y}(x, y; x', y') = & \sum_{p=1}^{\infty} \sum_{q=1}^{\infty} C_1 (k_x k_y) \cos(k_x x) \\ & \times \sin(k_x x') \sin(k_y y) \cos(k_y y') \quad (20) \end{aligned}$$

$$\begin{aligned} G_{M_y}^{H_y}(x, y; x', y') = & - \sum_{p=0}^{\infty} \sum_{q=1}^{\infty} C_1 \epsilon_p (k_0^2 - k_y^2) \cos(k_x x) \\ & \times \cos(k_x x') \sin(k_y y) \sin(k_y y') \quad (21) \end{aligned}$$

where

$$C_1 = \frac{2}{j\omega\mu_0 abk_g \tan(k_g c)} \quad (22)$$

$$k_x = \frac{p\pi}{a}, \quad k_y = \frac{q\pi}{b}, \quad k_g = \sqrt{k_0^2 - k_x^2 - k_y^2} \quad (23)$$

and  $\epsilon_{p,q}$  are Neumann's number (1 for  $p, q = 0$  and 2 for  $p, q > 0$ ). In implementing (18)–(21) numerically, the summations are truncated at  $p = P$  and  $q = Q$ .

#### B. Evaluation of $Y_{mn}^c$

To evaluate  $Y_{mn}^c$ , a large number of cavity modes are needed for the function to converge. Integrating  $Y_{mn}^c$  numerically takes a long time to obtain a satisfactory result. To save computation time, the integration is done analytically. It is found that the admittance integrals for  $G_{M_\alpha}^{H_\beta}(\alpha, \beta = x, y)$  can be expressed as products of two double integrals. The generalized form for the double integrals is given as follows:

$$\begin{aligned} & \int_{\xi=-W}^W \int_{\eta=\eta_i-d}^{\eta_i+d} \sin(a_1 + b_1 \xi + c_1 \eta) \cos(a_2 + b_2 \xi + c_2 \eta) \\ & \times \sin[k_e(d - |\eta - \eta_i|)] d\xi d\eta \\ & = \sum_{t=-1,1} \frac{2k_e \sin[(b_1 + tb_2)W]}{(b_1 + tb_2)[(c_1 + tc_2)^2 - k_e^2]} \{ \cos(k_e d) \\ & - \cos[(c_1 + tc_2)d] \} \sin[(a_1 + ta_2) + (c_1 + tc_2)\eta_i] \quad (24) \end{aligned}$$

where  $a_i, b_i$  and  $c_i$  are constants. Note that there is a singularity at  $(b_1 + tb_2) = 0$ , which is handled in the program by using  $\lim_{x \rightarrow 0} (\sin x / x) = 1$ .

## IV. COMPUTED AND MEASURED RESULTS

To verify the theory, four cavity-backed slot-excited hemispherical DRA's (Antennas I–IV) were constructed. Antenna I is used to show the feasibility of this antenna configuration, whereas Antennas II–IV are used to study cavity resonances and the effect of the slot inclination angle  $\phi_{\text{in}}$ . Antenna I has a slot of length  $L = 1.54$  cm and width  $W = 0.5$  mm and a cavity of width  $a = 2.11$  cm, length  $b = 3.38$  cm, and depth  $c = 4.6$  cm. The slot inclination angle is  $\phi_{\text{in}} = 90^\circ$ . In Antennas II–IV, a slot of length  $L = 1.8$  cm and width  $W = 0.6$  mm and a cavity of width  $a = 4.24$  cm, length  $b = 7.41$  cm, and depth  $c = 10.1$  cm were fabricated. The slot inclination angles in Antennas II–IV are  $0, 90^\circ$  and  $45^\circ$  respectively. In each antenna, a ground plane of size  $15 \times 15$  cm<sup>2</sup> and thickness 0.1 mm was made by sticking adhesive conducting tapes onto a foam board. The slot cut from the ground plane was excited by a semi-rigid cable RG402 of outer radius  $r_1 = 3.6$  mm and inner radius  $r_2 = 0.9$  mm, which coupled energy to the cavity and DRA. The semi-rigid cable penetrated the cavity and lay on the ground plane. The DRA is of radius  $a_r = 1.25$  cm and dielectric constant  $\epsilon_r = 9.5$ . To solve the air-gap problem, the DRA was mounted tightly onto the adhesive side of the tapes to remove any possible air gap between itself and the ground plane. The slot is located at the center of the DRA to maximize the coupling for the DRA TE<sub>111</sub> mode. The measurements were taken using an HP8510C network analyzer.

To check the convergence of the theory, the input impedance is calculated using various modal terms  $P$  and  $Q$  for the Green's function  $G_c$ . A bad case is considered which requires more modal terms to converge. Since more modal terms are needed for a larger cavity, Antenna III instead of Antenna I is selected. Moreover, we take  $x_d = a/8$  so that the slot is not at the center of the cavity. In this case, both TE and TM

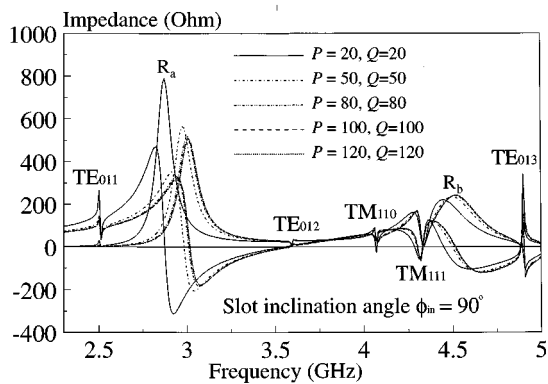
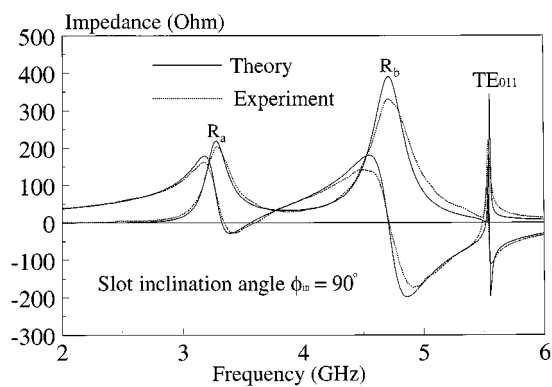
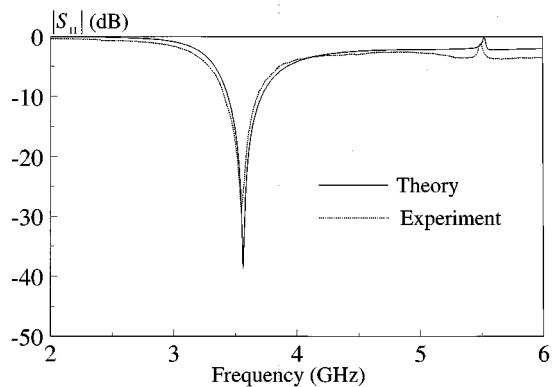


Fig. 2. Convergence check of the modal solution  $G_c$ :  $\phi_{in} = 90^\circ$ ,  $L = 1.80$  cm,  $W = 0.6$  mm,  $a_r = 1.25$  cm,  $\epsilon_r = 9.5$ ,  $a = 4.24$  cm,  $b = 7.41$  cm,  $c = 10.1$  cm,  $x_d = 5.3$  mm, and  $y_d = b/2$ .



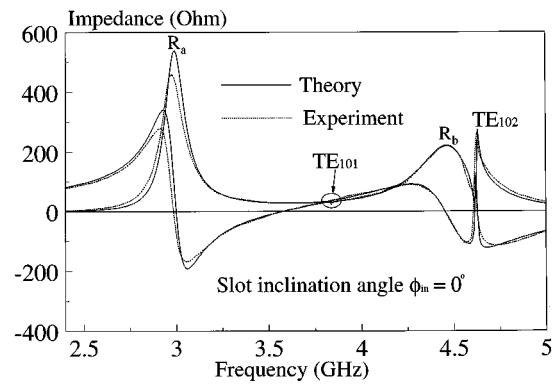
(a)



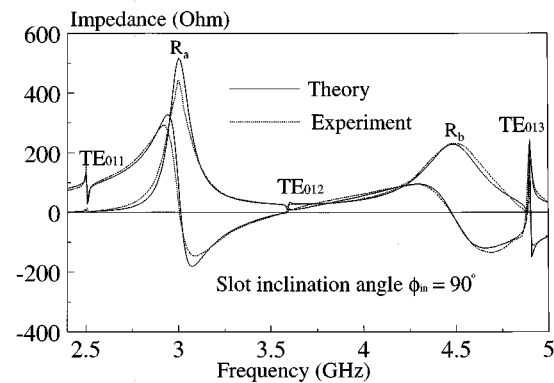
(b)

Fig. 3. Measured and calculated results:  $\phi_{in} = 90^\circ$ ,  $L = 1.54$  cm,  $W = 0.5$  mm,  $a_r = 1.25$  cm,  $\epsilon_r = 9.5$ ,  $a = 2.11$  cm,  $b = 3.38$  cm,  $c = 4.6$  cm,  $x_d = a/2$ , and  $y_d = b/2$ . (a) Input impedance. (b) Return loss.

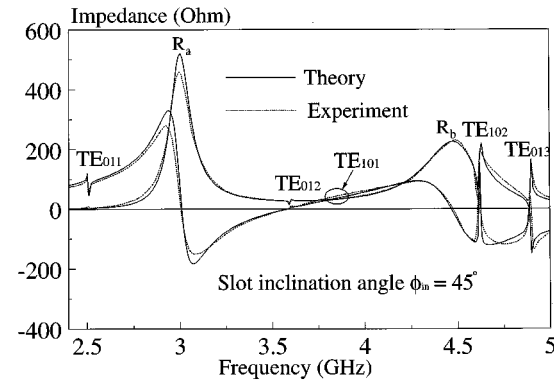
modes of the cavity are excited and many more modal terms are required for the solution to converge. The results are shown in Fig. 2 where it is found that  $P = Q = 100$  gives a very good result for this antenna configuration, but to further ensure the convergence,  $P = Q = 120$  are used in the following calculations. For  $G_a$ , it was found that [8] using 15 modal terms is sufficient to obtain a converged result. The computations were carried out on a Digital Alpha Workstation 250. It took about 15 min for a single data point by using the Gaussian numerical integration, while it took only 18 s by using the



(a)



(b)



(c)

Fig. 4. Measured and calculated input impedances against frequency for different slot inclination angles:  $L = 1.80$  cm,  $W = 0.6$  mm,  $a_r = 1.25$  cm,  $\epsilon_r = 9.5$ ,  $a = 4.24$  cm,  $b = 7.41$  cm,  $c = 10.1$  cm,  $x_d = a/2$ , and  $y_d = b/2$ . (a)  $\phi_{in} = 0^\circ$ . (b)  $\phi_{in} = 90^\circ$ . (c)  $\phi_{in} = 45^\circ$ .

analytical result (24). With reference to Fig. 2, several resonances are observed which are labeled in the figure. The first, second, and third indexes refer to the  $x$ -,  $y$ -, and  $z$ -variations, respectively. It should be noted that the natural resonances of the cavity occur at the minimum resistance points [13], [16]. This is because at the natural resonances of the cavity, the tangential electric field in the slot is almost zero, giving a very small input resistance. The cavity  $TE_{mnr}$ - and  $TM_{mnr}$ -mode natural resonant frequencies can be predicted accurately by using  $(f_r)_{mnr}^{TE, TM} = \sqrt{(m/a)^2 + (n/b)^2 + (r/c)^2} / (2\sqrt{\epsilon_0\mu_0})$  [18]. Using this simple formula, the natural resonances of the cavity  $TE_{011}$ ,  $TE_{012}$ ,  $TM_{110}$ ,  $TM_{111}$ , and  $TE_{013}$  modes are

TABLE I  
MEASURED AND CALCULATED RESONANT FREQUENCIES IN FIG. 4. THE  $TE_{101}$  MODE IS TOO WEAK TO MEASURE. (a)  $\phi_{in} = 0^\circ$  CORRESPONDING TO FIG. 4(a).  
(b)  $\phi_{in} = 90^\circ$  CORRESPONDING TO FIG. 4(b). (c)  $\phi_{in} = 45^\circ$  CORRESPONDING TO FIG. 4(c)

	Theory (GHz)	Experiment (GHz)	Error (%)	Simple formula (GHz)
$R_a$ (zero reactance)	3.00	2.99	0.33	—
$TE_{101}$ (min. resistance)	3.84	3.84	0.00	3.84
$R_b$ (zero reactance)	4.45	4.45	0.00	—
$TE_{102}$ (min. resistance)	4.61	4.61	0.00	4.62
$TE_{102}$ (zero reactance)	4.63	4.63	0.00	—

(a)

	Theory (GHz)	Experiment (GHz)	Error (%)	Simple formula (GHz)
$TE_{011}$ (min. resistance)	2.51	2.51	0.00	2.51
$R_a$ (zero reactance)	3.01	3.01	0.00	—
$TE_{012}$ (min. resistance)	3.59	3.59	0.00	3.59
$R_b$ (zero reactance)	4.48	4.48	0.00	—
$TE_{013}$ (min. resistance)	4.89	4.88	0.20	4.89
$TE_{013}$ (zero reactance)	4.91	4.91	0.00	—

(b)

	Theory (GHz)	Experiment (GHz)	Error (%)	Simple formula (GHz)
$TE_{011}$ (min. resistance)	2.51	2.52	0.40	2.51
$R_a$ (zero reactance)	3.01	3.01	0.00	—
$TE_{012}$ (min. resistance)	3.59	3.60	0.27	3.59
$TE_{101}$ (min. resistance)	3.84	—	—	3.84
$R_b$ (zero reactance)	4.47	4.48	0.22	—
$TE_{102}$ (min. resistance)	4.61	4.61	0.00	4.62
$TE_{102}$ (zero reactance)	4.63	4.63	0.00	—
$TE_{013}$ (min. resistance)	4.89	4.89	0.00	4.89
$TE_{013}$ (zero reactance)	4.90	4.90	0.00	—

(c)

found to be 2.51, 3.59, 4.08, 4.34, and 4.89 GHz, respectively, which are exactly the same as those at the minimum resistance points in Fig. 2. The resonances  $R_a$  and  $R_b$  are due to the coupling between the slot and the DRA  $TE_{111}$  mode. Note that the frequencies differ from the source-free values (3.38 GHz for the slot and 3.68 GHz for the DRA) because the slot and DRA modes are affected by each other and influenced by the nearby cavity modes. A similar phenomenon was observed in [1] when there were two closely spaced DRA resonant modes.

The measured and calculated input impedances of Antenna I are displayed in Fig. 3(a), where a reasonable agreement

between theory and experiment is observed. Three peaks are found, namely  $R_a$ ,  $R_b$ , and the cavity  $TE_{011}$  mode. The measured forced resonant frequencies (zero reactance) of  $R_a$ ,  $R_b$ , and the cavity  $TE_{011}$  mode are 3.34, 4.72, and 5.54 GHz, respectively, whereas the corresponding calculated values are 3.32, 4.71, and 5.55 GHz. The errors are less than 1%. For the natural resonance of the cavity  $TE_{011}$  mode, the measured and calculated frequencies (minimum resistance) are 5.48 and 5.52 GHz (0.73% error), respectively, which agree very well with the predicted value of 5.51 GHz using the simple formula. In actual applications, the return loss is of practical

interest. The measured and calculated return losses of Antenna I are shown in Fig. 3(b), where it is observed that a very good impedance match is achieved for the configuration. The measured and calculated resonant frequencies ( $\min |S_{11}|$ ) are 3.55 and 3.56 GHz (0.28% error), respectively, which are now very close to the DRA source-free value of 3.68 GHz. A similar phenomenon has been observed in the aperture-coupled DRA [8]. The measured and calculated bandwidths ( $|S_{11}| < -10$  dB) are 7.48 and 7.55%, respectively, which are very close to that of the aperture-coupled DRA [19]. As seen from the figure, a resonant mode due to the cavity  $TE_{111}$  mode is observed around 5.5 GHz. The cavity mode, however, does not affect the DRA resonance very much, as desired in practical applications.

Next we investigate Antennas II–IV to see other cavity resonances and the effect of the slot inclination angle. Fig. 4 shows the measured and calculated input impedances of the antennas. As can be observed from the figure, good agreement between theory and experiment is obtained. The calculated and measured resonant frequencies are summarized in Table I, where the results using the simple formula are also given. With reference to Fig. 4, the  $R_a$  and  $R_b$  resonances are not affected significantly by the slot inclination angle. Conversely, the cavity modes are strongly affected by the slot inclination angle, as expected. Comparing Fig. 4(a) with Fig. 4(b), it is observed that only  $TE_{10r}$  ( $r = 1, 2$ ) modes are excited when the slot inclination angle is zero ( $\phi_{in} = 0$ ), while only  $TE_{01r'}$  ( $r' = 1, 2, 3$ ) modes are excited when  $\phi_{in} = 90^\circ$ . When  $\phi_{in} = 45^\circ$  (Fig. 4(c)), both  $TE_{10r}$  and  $TE_{01r'}$  modes are excited. Note that no cavity TM modes can be excited since the slot is now located at the center of the cavity (i.e.,  $x_d = a/2$ ,  $y_d = b/2$ ).

Fig. 5 shows the peak resistance of  $R_a$  in Fig. 4(a) as a function of the slot inclination angle  $\phi_{in}$ . With reference to the figure, the peak resistance decreases from 540 to 516  $\Omega$  as  $\phi_{in}$  increases from  $0^\circ$  to  $90^\circ$ . The deviation is about 4.5%. The corresponding resonant frequency (zero reactance) of the peak as a function  $\phi_{in}$  was also plotted but the frequency was found to remain nearly constant as observed in Table I(a)–(c).

Fig. 6 shows the calculated input impedance of the antenna for  $c = 8.0, 9.0$ , and  $10.1$  cm, with  $\phi_{in}$  set to  $90^\circ$ . With reference to the figure, the cavity depth  $c$  mainly affects the cavity resonance; the deeper the cavity is, the lower the resonant frequency, as expected. It was found that the natural resonant frequencies of the cavity were accurately predicted by the simple formula.

Fig. 7 shows the calculated input impedance of the antenna for  $x_d = 0.53, 1.06$ , and  $2.12$  cm, with  $\phi_{in} = 90^\circ$ . It is seen from the figure that the slot offset restores the  $TM_{11r}$  ( $r = 1, 2$ ) modes. Observe that the resonance  $R_b$  is affected strongly by the  $TM_{111}$  mode. Once again, all the natural resonant frequencies of the cavity can be predicted very accurately by the simple formula.

Fig. 8 shows the calculated input impedance of the antenna as a function of frequency for  $y_d = 1.50, 2.60$  and  $3.71$  cm, with  $\phi_{in} = 90^\circ$ . Unlike the previous case in which both cavity TE and TM modes are excited, the offset  $y_d$  can only excite cavity TE modes. It is noted that  $y_d$  excites an additional cavity mode, the  $TE_{021}$  mode, which cannot be found when the slot is placed at the center of the cavity.

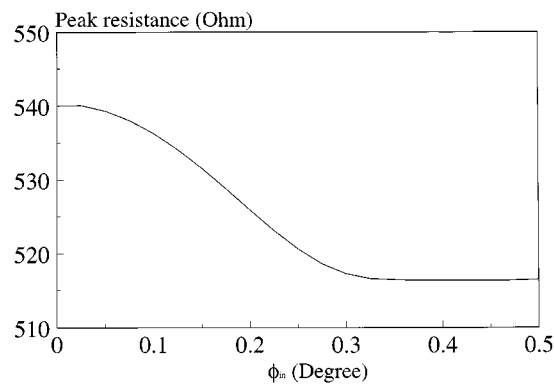


Fig. 5. Input resistance of the first resonance against the slot inclination angle  $\phi_{in}$ . The parameters are the same as Fig. 4(a).

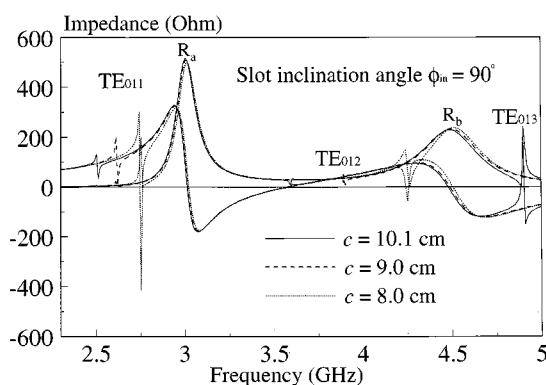


Fig. 6. Calculated input impedance against frequency for different cavity depths  $c = 8.0, 9.0$ , and  $10.1$  cm. Other parameters are the same as Fig. 4(b).

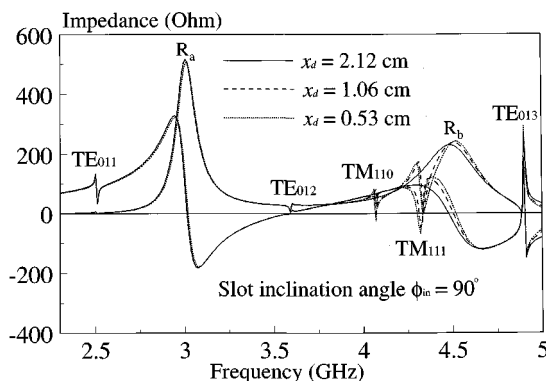


Fig. 7. Calculated input impedance against frequency for different slot offsets  $x_d = 0.53, 1.06$ , and  $2.12$  cm. Other parameters are the same as Fig. 4(b).

The magnetic currents in Fig. 4(a) are shown in Fig. 9. As the  $TE_{101}$  mode is too weak, it is not considered here. Due to the symmetry of the current, only the positive half ( $0 \leq y \leq L/2$ ) is shown in the figure. With reference to the Fig. 9(a), the current at the first resonance ( $f_r = 3.00$  GHz, zero reactance) has the largest amplitude. The currents of  $R_a$ ,  $R_b$ , and  $TE_{102}$  mode have a typical resonant waveform, as expected. Note that the amplitude of the current at the natural ( $TE_{102}$ ) resonant mode is relatively small, which was previously found in the hemispherical cavity-backed slot antenna [13]. Fig. 9(b) shows the phase of the magnetic current. It is found that the phase is zero at  $y = 0$  for

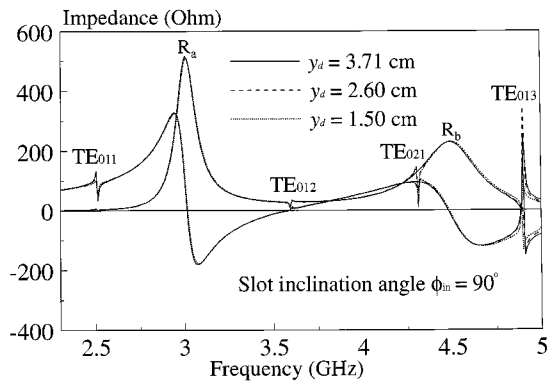


Fig. 8. Calculated input impedance against frequency for different slot offsets  $y_d = 1.50, 2.60,$  and  $3.71$  cm. Other parameters are the same as Fig. 4(b).

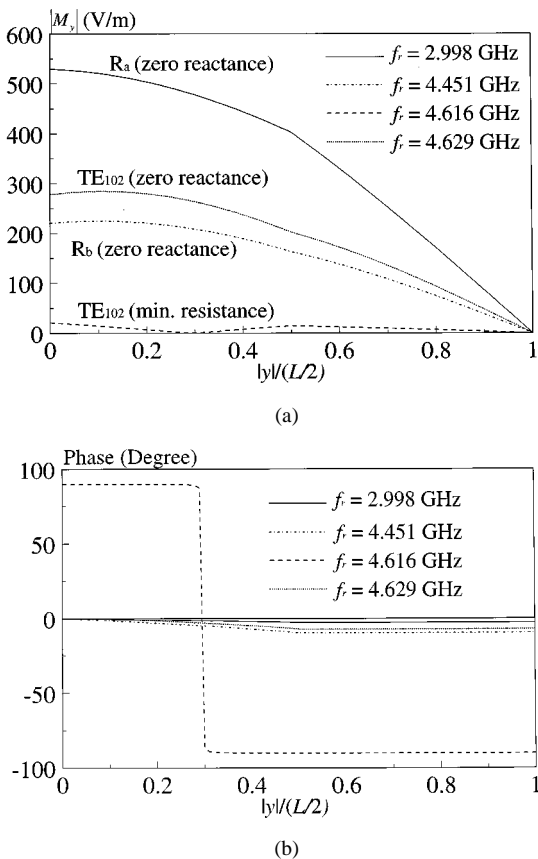


Fig. 9. Calculated equivalent magnetic current in the slot. The parameters are the same as Fig. 4(a). (a) Magnitude. (b) Phase.

$f_r = 3.0, 4.45,$  and  $4.63$  GHz, causing the input impedance to be purely real at these frequencies. The phase at these frequencies decreases gradually along the slot. In contrast, the phase at  $y = 0$  is  $90^\circ$  for  $f_r = 4.62$  GHz and, hence, the input resistance at this frequency is almost zero. In other words, the energy is reactive and cannot be radiated. Moreover, at this frequency a  $180^\circ$  phase change at  $|y|/(L/2) = 0.3$  is also observed and the current forms two parts (totally three parts along the whole slot) in opposite directions. Unlike the other three cases ( $f_r = 3.0, 4.45,$  and  $4.63$  GHz), there is no net radiation at this frequency

as the far fields radiated by the antiphase current segments are cancelled out.

## V. CONCLUSION

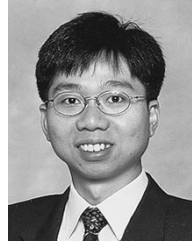
The input impedance of the cavity-backed slot-excited DRA antenna has been studied theoretically and experimentally. The Green's function technique and moment method have been used to solve the problem. The integration of the cavity admittances has been done analytically to speed the computation. To demonstrate the feasibility of the antenna configuration, the dimensions of the cavity are so chosen that there are no cavity resonant modes around the DRA  $TE_{111}$  mode. An excellent impedance match has been achieved.

The second part of the study is to investigate the cavity resonances with the presence of the DRA. In this case, the cavity resonances are near the DRA resonance. The input impedance of the antenna has been measured and calculated for different slot inclination angles. Good agreement between theory and experiment has been obtained. It has been found that the inclination angle can be used to change the impedance level of the first resonance by a few percent, while the resonant frequency remains almost unchanged. The effects of the cavity depth and of the slot position on the input impedance have been studied. It has been observed that all excited cavity resonances are TE modes when  $x_d = a/2$ , otherwise TM modes are also excited. Finally, the magnitude and phase of the magnetic currents in the slot have been discussed for different resonant modes. It has been found that the DRA and forced cavity resonant modes can radiate but the natural cavity resonant mode cannot, as expected.

## REFERENCES

- [1] S. A. Long, M. W. McAllister, and L. C. Shen, "The resonant cylindrical dielectric resonator antenna," *IEEE Trans. Antennas Propagat.*, vol. 31, pp. 406–412, May 1983.
- [2] M. W. McAllister, S. A. Long, and G. L. Conway, "Rectangular dielectric resonator antenna," *Electron. Lett.*, vol. 19, pp. 218–219, 1983.
- [3] M. W. McAllister and S. A. Long, "Resonant hemispherical dielectric antenna," *Electron. Lett.*, vol. 20, pp. 657–658, 1984.
- [4] R. A. Kranenburg and S. A. Long, "Microstrip transmission line excitation of dielectric resonator antennas," *Electron. Lett.*, vol. 24, pp. 1156–1157, 1988.
- [5] —, "Coplanar waveguide excitation of dielectric resonator antennas," *IEEE Trans. Antennas Propagat.*, vol. 39, pp. 119–122, Jan. 1991.
- [6] A. A. Kishk, G. Zhou, and A. W. Glisson, "Analysis of dielectric resonator antennas with emphasis on hemispherical structures," *IEEE Antennas Propagat. Mag.*, vol. 36, pp. 20–31, Apr. 1994.
- [7] K. W. Leung, K. M. Luk, K. Y. A. Lai, and D. Lin, "Theory and experiment of probe fed dielectric resonator antenna," *IEEE Trans. Antennas Propagat.*, vol. 41, pp. 1390–1398, Oct. 1993.
- [8] —, "Theory and experiment of an aperture-coupled hemispherical dielectric resonator antenna," *IEEE Trans. Antennas Propagat.*, vol. 43, pp. 1192–1198, Nov. 1995.
- [9] J. Galejs, "Admittance of a rectangular slot which is backed by a rectangular cavity," *IEEE Trans. Antennas Propagat.*, vol. AP-11, pp. 119–126, Mar. 1963.
- [10] C. R. Cockrell, "The input admittance of the rectangular cavity-backed slot antenna," *IEEE Trans. Antennas Propagat.*, vol. AP-24, pp. 288–294, May 1976.
- [11] M. Li, K. A. Hummer, and K. Chang, "Theoretical and experimental study of the input impedance of the cylindrical cavity-backed rectangular slot antenna," *IEEE Trans. Antennas Propagat.*, vol. 39, pp. 1158–1166, Aug. 1991.
- [12] A. Hadidi and M. Hamid, "Aperture field and circuit parameters of cavity-backed slot radiator," *Proc. Inst. Elect. Eng.*, pt. H, vol. 136, pp. 139–146, Apr. 1989.

- [13] K. W. Leung and K. Y. Chow, "Theory and experiment of the hemispherical cavity-backed slot antenna," *IEEE Trans. Antennas Propagat.*, vol. 46, pp. 1234–1241, Aug. 1998.
- [14] S. A. Long, "Experimental study of the impedance of cavity-backed slot antennas," *IEEE Trans. Antennas Propagat.*, vol. 23, pp. 1–7, Jan. 1975.
- [15] —, "A mathematical model for the impedance of the cavity-backed slot antenna," *IEEE Trans. Antennas Propagat.*, vol. 25, pp. 829–833, Nov. 1977.
- [16] E. M. Biebl and G. L. Friedsam, "Cavity-backed aperture antennas with dielectric and magnetic overlay," *IEEE Trans. Antennas Propagat.*, vol. 43, pp. 1226–1232, Nov. 1995.
- [17] C. T. Tai, *Dyadic Green's Function in Electromagnetic Theory*. Scranton, PA: Intext, 1972.
- [18] R. F. Harrington, *Time-Harmonic Electromagnetic Fields*. New York: McGraw-Hill, 1961.
- [19] K. W. Leung, "Rigorous analysis of dielectric resonator antenna using the method of moments," Ph.D. dissertation, Chinese Univ. Hong Kong, May 1993.



**Kwok Wa Leung** (S'90–M'93) was born in Hong Kong on April 11, 1967. He received the B.Sc. (electronics) and Ph.D. (electronic engineering) degrees from the Chinese University of Hong Kong, Shatin, Hong Kong, in 1990 and 1993, respectively.

From 1990 to 1993, he was a Graduate Assistant in the Department of Electronic Engineering, Chinese University of Hong Kong. He joined the Department of Electronic Engineering, City University of Hong Kong, in 1994 as an Assistant Professor and became an Associate Professor in 1999. His research interests include dielectric resonator antennas, microstrip antennas, wire antennas, numerical methods in electromagnetics, and mobile communications.



**Kut Yuen Chow** was born in Guangdong Province, China, on August 25, 1971. He received the B.Eng. and Ph.D. degrees in electronic engineering from the City University of Hong Kong, in 1995 and 1999, respectively.

He has worked as a Senior Research Assistant in the Department of Electronic Engineering, City University of Hong Kong from September to December 1999. Since 2000 he has been an RF Engineer with Philips Semiconductors-Electronic Devices Limited. His current research interests include the wireless

communication systems, electromagnetic theory, and microwave measurement techniques.